Available online at http://jprm.sms.edu.pk/
Journal of Prime Research in Mathematics, 17(1) (2021), 95–114

Journal of Prime Research in Mathematics

A cubic trigonometric B-spline collocation method based on Hermite formula for the numerical solution of the heat equation with classical and non-classical boundary conditions

Aatika Yousaf[a], Muhammad Yaseen[a,*]

[a]Department of Mathematics, University of Sargodha,40100, Sargodha, Pakistan.

Abstract

In this article, a new trigonometric cubic B-spline collocation method based on the Hermite formula is presented for the numerical solution of the heat equation with classical and non-classical boundary conditions. This scheme depends on the standard finite difference scheme to discretize the time derivative while cubic trigonometric B-splines are utilized to discretize the derivatives in space. The scheme is further refined utilizing the Hermite formula. The stability analysis of the scheme is established by standard Von-Neumann method. The numerical solution is obtained as a piecewise smooth function empowering us to find approximations at any location in the domain. The relevance of the method is checked by some test problems. The suitability and exactness of the proposed method are shown by computing the error norms. Numerical results are compared with some current numerical procedures to show the effectiveness of the proposed scheme.

Keywords: Heat equation, cubic B-splines collocation method, cubic trigonometric basis function, Hermite formula, stability.
2010 MSC: 65M70, 65Z05, 65D05, 65D07, 35B35.

1. Introduction

The heat equation is of central significance in various scientific fields and it is responsible to govern the temperature distribution across some domain and some dimension. The heat equation is given as

$$\frac{\partial v}{\partial t} = \nu^2 \frac{\partial^2 v}{\partial s^2} + g(s,t), \quad c \le s \le d, \quad t > 0, \tag{1.1}$$

*Corresponding author
Email addresses: aatika.yousaf101@gmail.com (Aatika Yousaf), yaseen.yaqoob@uos.edu.pk (Muhammad Yaseen)

Received : 5 March 2020*; Accepted:* 5 November 2020*; Published Online:* 30 June 2021.

where ν is the diffusivity of the rod and is dependent on the thermal conductivity, density and the specific heat of the rod. The Eq. (1.1) is subject to the following initial condition:

$$v(s,0) = \phi(s), \quad c \leq s \leq d \tag{1.2}$$

and the following classical and non classical boundary conditions:

$$\begin{cases} v(c,t) = \alpha(t), \\ v(d,t) = \beta(t), \end{cases} \qquad t > 0 \tag{1.3}$$

$$\begin{cases} v(c,t) = \int_c^d \psi_1(s) v(s,t) ds, \\ v(d,t) = \int_c^d \psi_2(s) v(s,t) ds, \end{cases} \qquad t > 0 \tag{1.4}$$

respectively. Here, α, β are assumed to be smooth functions of t.

Numerous physical processes are modeled by non-classical boundary conditions. Researchers have shown great interest in partial differential equations with non-classical boundary conditions. Cahlon, Kulkarni and Shi [6] discussed stability analysis of a difference scheme for the heat equation with an integral constraint. Parabolic problems with non-classical boundary conditions in reproducing kernel space were solved by Zhou, Cui and Lin [23]. Dehghan [7] presented several difference schemes for the heat equation subject to nonlocal specifications. Further Dehghan [8] applied three new implicit difference schemes to the heat equation with boundary integral specifications. Golbabai and Javidi [12] introduced a numerical procedure dependent on local interpolating functions and Chebyshev polynomials for the heat equation with non-classical boundary conditions. Caglar [5] used cubic B-Splines to approximate the solution of the heat equation. Sun and Zhang [20] soled the heat equation using a compact high order boundary value method. Tatari and Dehghan [21] solved the heat equation via radial basis function. A comparison between the traditional separation of variables and Adomian decomposition method for the heat equation was presented by Gorguis and Benny Chan [13]. A one-dimensional heat equation was solved by Khabir [16] using a cubic B-spline collocation approach. Mohebbi and Dehghan [19] presented a fourth-order compact finite difference approximation and cubic C^1-spline collocation method for the numerical solution of the heat equation with fourth-order accuracy in both space and time variables. In literature, Kumar [18] concluded that the spline approach is much more efficient than the finite difference schemes applied to boundary value problems. Consequently, this approach had been of preference to many authors [3, 14, 24, 25].

In this study, the Hermite formula is applied in a cubic trigonometric B-spline col- location scheme in order to derive the approximate solution of the heat equation. Von Neumann method is utilized to affirm that the given scheme is stable unconditionally. Various numerical results are being derived out and the results are compared with those results presented in [9, 10, 11, 22, 2].

The remaining portion of the paper is arranged in the following sequence. The Section 2 of this paper comprises of the proposed scheme which is derived out for the numerical treatment of heat equation. Later on in Section **??**, the stability of the scheme is talked about. The comparison of numerical results is manifested in Section **??**. Section **??** presents the conclusion of this study.

2. Derivation of the Scheme

Let $t = \frac{T}{k}$ and $h = \frac{b-a}{M}$ be the time and space step sizes respectively. Let $t_n = nk,\ n = 0, 1, 2, ..., N$, $s_j = jh,\ j = 0, 1, 2...M$. The solution domain $c \leq s \leq d$ is equally divided by knots s_j into M equal subintervals $[s_j, s_{j+1}]$, $j = 0, 1, 2, ..., M-1$, where $c = s_0 < s_1 < ... < s_{n-1} < s_M = d$. The scheme requires approximate solution $V(s,t)$ to the exact solution $v(s,t)$ in the form [1]:

$$V(s,t) = \sum_{j=-3}^{M-1} D_j(t) TB_j^4(s), \tag{2.1}$$

where $D_j(t)$ are unknowns to be found and the cubic trigonometric B-splines, $TB_j^4(s)$ are given by [1]:

$$TB_j^4(s) = \frac{1}{p}\begin{cases} l^3(s_j), & s \in [s_j, s_{j+1}], \\ l(s_j)(l(s_j)m(s_{j+2}) + m(s_{j+3})l(s_{j+1})) + m(s_{j+4})l^2(s_{j+1}), & s \in [s_{j+1}, s_{j+2}], \\ m(s_{j+4})(l(s_{j+1})m(s_{j+3}) + m(s_{j+4})l(s_{j+2})) + l(s_j)m^2(s_{j+3}), & s \in [s_{j+2}, s_{j+3}], \\ m^3(s_{j+4}), & s \in [s_{j+3}, s_{j+4}], \end{cases} \tag{2.2}$$

where $l(s_j) = \sin\left(\frac{s - s_j}{2}\right)$, $m(s_j) = \sin\left(\frac{s_j - s}{2}\right)$, $p = \sin\left(\frac{h}{2}\right)\sin(h)\sin\left(\frac{3h}{2}\right)$. Here, $TB_{j-3}^4(s), TB_{j-2}^4(s)$ and $TB_{j-1}^4(s)$ are survived due to local support characteristic of the cubic B-splines so that the approximation v_j^n at the grid point (s_j, t_n) at n^{th} time level is given as

$$v(s_j, t^n) = v_j^n = \sum_{w=j-3}^{j-1} D_j^n(t) TB_j^4(s). \tag{2.3}$$

Initial and boundary conditions of the given equation and the collocation conditions on $B_j^3(s)$ are utilized to find the time dependent unknowns $c_j^n(t)$. Consequently, the approximations v_j^n and its necessary derivatives are found as:

$$\begin{cases} v_j^n = \zeta_1 D_{j-3}^n + \zeta_2 D_{j-2}^n + \zeta_1 D_{j-1}^n, \\ (v_s)_j^n = -\zeta_3 D_{j-3}^n + \zeta_3 D_{j-1}^n, \\ (v_{ss})_j^n = \zeta_5 D_{j-3}^n + \zeta_6 D_{j-2}^n + \zeta_5 D_{j-1}^n, \end{cases} \tag{2.4}$$

where $\zeta_1 = \csc(h)\csc\left(\frac{3h}{2}\right)\sin^2\left(\frac{h}{2}\right)$, $\zeta_2 = \frac{2}{1 + 2\cos(h)}$, $\zeta_3 = \frac{3}{4}\csc\left(\frac{3h}{2}\right)$, $\zeta_5 = \frac{3 + 9\cos(h)}{4\cos\left(\frac{h}{2}\right) - 4\cos\left(\frac{5h}{2}\right)}$, $\zeta_6 = -\frac{3\cot^2\left(\frac{h}{2}\right)}{2 + 4\cos(h)}$. The Hermite formula [17] is given as:

$$\frac{\partial^2 v(s_{j-1}, t_n)}{\partial s^2} + 10\frac{\partial^2 v(s_j, t_n)}{\partial s^2} + \frac{\partial^2 v(s_{j+1}, t_n)}{\partial s^2} - \frac{12}{h^2}(v(s_{j-1}, t_n) - 2v(s_j, t_n) + v(s_{j+1}, t_n)) = 0. \tag{2.5}$$

Substituting (2.4) in (2.5) and denoting $v(s_j, t_n)$ by v_j^n, we obtain

$$(v_{ss})_j^n = -\frac{1}{10}(v_{ss})_{j-1}^n - \frac{1}{10}(v_{ss})_{j+1}^n + \frac{6}{5h^2}(v_{j-1}^n - 2v_j^n + v_{j+1}^n). \tag{2.6}$$

Substituting (2.4) in (2.6), we obtain

$$(v_{ss})_j^n = \omega_1 D_{j-4}^n + \omega_2 D_{j-3}^n + \omega_3 D_{j-2}^n + \omega_2 D_{j-1}^n + \omega_1 D_j^n, \tag{2.7}$$

where $\omega_1 = \frac{-\zeta_5}{10} + \frac{6\zeta_1}{5h^2}$, $\omega_2 = \frac{-\zeta_6}{10} - \frac{12\zeta_1}{5h^2} + \frac{6\zeta_2}{5h^2}$, $\omega_3 = \frac{-\zeta_5}{5} + \frac{12\zeta_1}{5h^2} - \frac{12\zeta_2}{5h^2}$. The weighted θ-scheme is applied to the problem (2.1) to acquire

$$(v_t)_j^n = \theta h_j^{n+1} + (1 - \theta)h_j^n + g(s_j, t_{n+1}), \tag{2.8}$$

where $h_j^n = \nu^2(v_{ss})_j^n$ and $n = 0, 1, 2, 3, ...$ Now using the discretization $(v_t)_j^n = \frac{v_j^{n+1} - v_j^n}{k}$ in (2.8) and simplifying, we obtain

$$v_j^{n+1} - k\nu^2\theta(v_{ss})_j^{n+1} = v_j^n + k\nu^2(1 - \theta)(v_{ss})_j^n + kg(s_j, t_{n+1}). \tag{2.9}$$

Observe that the system (2.9) reduces to an explicit scheme, Crank-Nicolson scheme and a fully implicit scheme when $\theta = 0$, $\theta = \frac{1}{2}$ and $\theta = 1$ respectively. Here, the Crank-Nicolson approach is utilized so that (2.9) takes the form:

$$v_j^{n+1} - \frac{k\nu^2}{2}(v_{ss})_j^{n+1} = v_j^n + \frac{k\nu^2}{2}(v_{ss})_j^n + kg(s_j, t_{n+1}). \tag{2.10}$$

Substituting (2.4) in (2.10) and replacing j with $j-1$ yields:

$$\begin{aligned}&\left(\zeta_1 - \frac{k\nu^2\zeta_5}{2}\right) D_{j-4}^{n+1} + \left(\zeta_2 - \frac{k\nu^2\zeta_6}{2}\right) D_{j-3}^{n+1} + \left(\zeta_1 - \frac{k\nu^2\zeta_5}{2}\right) D_{j-2}^{n+1} \\ &= \left(\zeta_1 + \frac{k\nu^2\zeta_5}{2}\right) D_{j-4}^{n} + \left(\zeta_2 + \frac{k\nu^2\zeta_6}{2}\right) D_{j-3}^{n} + \left(\zeta_1 + \frac{k\nu^2\zeta_5}{2}\right) D_{j-2}^{n} + kg\left(s_j, t_{n+1}\right), \quad j = 0, M, \end{aligned} \tag{2.11}$$

Insert (2.4) and (2.7) in (2.10) to obtain

$$\begin{aligned}&-\left(\frac{k\nu^2\omega_1}{2}\right) D_{j-4}^{n+1} + \left(\zeta_1 - \frac{k\nu^2\omega_2}{2}\right) D_{j-3}^{n+1} + \left(\zeta_2 - \frac{k\nu^2\omega_3}{2}\right) D_{j-2}^{n+1} + \left(\zeta_1 - \frac{k\nu^2\omega_2}{2}\right) D_{j-1}^{n+1} - \left(\frac{k\nu^2\omega_1}{2}\right) D_{j}^{n+1} \\ &= \left(\frac{k\nu^2\omega_1}{2}\right) D_{j-4}^{n} + \left(\zeta_1 + \frac{k\nu^2\omega_2}{2}\right) D_{j-3}^{n} + \left(\zeta_2 + \frac{k\nu^2\omega_3}{2}\right) D_{j-2}^{n} + \left(\zeta_1 + \frac{k\nu^2\omega_2}{2}\right) D_{j-1}^{n} + \left(\frac{k\nu^2\omega_1}{2}\right) D_{j}^{n} \\ &\quad + kg\left(s_j, t_{n+1}\right), \qquad j = 1, 2, ..., M-1, \end{aligned} \tag{2.12}$$

Note that from (2.11) and (2.12), we obtain a system of $(M+1)$ equations in $(M+3)$ unknowns. To solve the system two additional equations are required which can be obtained using the given boundary conditions as:

$$\begin{cases} v_0^{n+1} = \alpha(t_{n+1}), & v_M^{n+1} = \beta(t_{n+1}) \\ \text{or} & \\ v_0^{n+1} = \int_c^d \psi_1(s_j)v(s_j, t_{n+1})ds, & v_M^{n+1} = \int_c^d \psi_2(s_j)v(s_j, t_{n+1})ds. \end{cases} \tag{2.13}$$

Consequently from (2.11), (2.12) and (2.13) a system of dimension $(M+3) \times (M+3)$ is found which can be numerically solved by using any numerical scheme based on Gaussian elimination.

Initial State: The initial condition and the derivatives of initial condition are used to find initial vector D^0 as given below

$$\begin{cases} (v_s)_j^0 = \phi'(s_j), & j = 0, \\ v_j^0 = \phi(s_j), & j = 0, 1, 2, ..., M, \\ (v_s)_j^0 = \phi'(s_j), & j = M. \end{cases} \tag{2.14}$$

The system (2.14) produces an $(M+3) \times (M+3)$ matrix system of the form

$$HD^0 = b, \tag{2.15}$$

where

$$H = \begin{bmatrix} -\zeta_3 & \zeta_4 & \zeta_3 & 0 & ... & 0 & 0 \\ \zeta_1 & \zeta_2 & \zeta_1 & 0 & ... & 0 & 0 \\ 0 & \zeta_1 & \zeta_2 & \zeta_1 & 0 & ... & 0 \\ \vdots & \vdots & \vdots & \vdots & \vdots & \vdots & \vdots \\ \vdots & \vdots & \vdots & \vdots & \vdots & \vdots & \vdots \\ \vdots & \vdots & \vdots & \vdots & \vdots & \vdots & \vdots \\ 0 & 0 & \dots & \dots & \zeta_1 & \zeta_2 & \zeta_1 \\ 0 & 0 & \dots & \dots & -\zeta_3 & \zeta_4 & \zeta_3 \end{bmatrix},$$

$D^0 = [D_{-4}^0, D_{-2}^0, D_{-1}^0, ..., D_{M-2}^0]$ and $b = [\phi'(s_0), \phi(s_0), ..., \phi(s_M), \phi'(s_M)]$.

3. Stability analysis

The Von Neumann stability technique is applied in this section to explore the stability of the given scheme. Consider the growth of error in a single Fourier mode $C_j^n = \delta^n e^{i\eta hj}$, where η is the mode number, h is the step size and $i = \sqrt{-1}$. Inserting the Fourier mode into equation (2.10) yields:

$$\begin{aligned} &-\rho_1\delta^{n+1}e^{i\eta h(j-4)} + \rho_2\delta^{n+1}e^{i\eta h(j-3)} + \rho_3\delta^{n+1}e^{i\eta h(j-2)} + \rho_2\delta^{n+1}e^{i\eta h(j-1)} - \rho_1\delta^{n+1}e^{i\eta h(j)} \\ &= \rho_1\delta^n e^{i\eta h(j-4)} + \rho_4\delta^n e^{i\eta h(j-3)} + \rho_5\delta^n e^{i\eta h(j-2)} + \rho_4\delta^n e^{i\eta h(j-1)} + \rho_1\delta^n e^{i\eta h(j)}, \end{aligned} \quad (3.1)$$

where, $\rho_1 = \frac{k\nu^2\omega_1}{2}$, $\rho_2 = \zeta_1 - \frac{k\nu^2\omega_2}{2}$, $\rho_3 = \zeta_2 - \frac{k\nu^2\omega_3}{2}$, $\rho_4 = \zeta_1 + \frac{k\nu^2\omega_2}{2}$, $\rho_5 = \zeta_2 + \frac{k\nu^2\omega_3}{2}$. Dividing Eq. (3.1) by $\delta^n e^{i\eta(j-2)h}$ and rearranging the equation, we obtain

$$\delta = \frac{\rho_1 e^{-2i\eta h} + \rho_4 e^{-i\eta h} + \rho_5 + \rho_4 e^{i\eta h} + \rho_1 e^{2i\eta h}}{-\rho_1 e^{-2i\eta h} + \rho_2 e^{-i\eta h} + \rho_3 + \rho_2 e^{i\eta h} - \rho_1 e^{2i\eta h}}. \quad (3.2)$$

Using $\cos(\eta h) = \frac{e^{i\eta h}+e^{-i\eta h}}{2}$ in Eq. (3.2) and simplifying, we obtain

$$\delta = \frac{2\rho_1 cos(2\eta h) + 2\rho_4 cos(\eta h) + \rho_5}{-2\rho_1 cos(2\eta h) + 2\rho_2 cos(\eta h) + \rho_3}, \quad (3.3)$$

Note that $\eta \in [-\pi, \pi]$. Without loss of generality, we can assume that $\eta = 0$, so that Eq. (3.3) takes the form:

$$\begin{aligned} \delta &= \frac{2\rho_1 + 2\rho_4 + \rho_5}{-2\rho_1 + 2\rho_2 + \rho_3}, \\ &= \frac{k\nu^2\omega_1 + 2\zeta_1 + k\nu^2\omega_2 + \zeta_2 + \frac{1}{2}k\nu^2\omega_3}{-k\nu^2\omega_1 + 2\zeta_1 - k\nu^2\omega_2 + \zeta_2 - \frac{1}{2}k\nu^2\omega_3}, \\ &= \frac{2\zeta_1 + \zeta_2 + k\nu^2(\omega_1 + \omega_2 + \frac{1}{2}\omega_3)}{2\zeta_1 + \zeta_2 - k\nu^2(\omega_1 + \omega_2 + \frac{1}{2}\omega_3)}. \end{aligned}$$

From (2) we have $\omega_1 + \omega_2 + \frac{1}{2}\omega_3 = -\frac{1}{5}\zeta_5 - \frac{1}{10}\zeta_6$, so

$$\delta = \frac{2\zeta_1 + \zeta_2 - \frac{1}{5}k\nu^2\zeta_5 - \frac{1}{10}k\nu^2\zeta_6}{2\zeta_1 + \zeta_2 + \frac{1}{5}k\nu^2\zeta_5 + \frac{1}{10}k\nu^2\zeta_6} \leq 1, \quad (3.4)$$

which proves that the present computational scheme is stable unconditionally.

4. Convergence analysis

In this section, we present the convergence analysis of the proposed scheme. For this purpose, we need to recall the following theorem [15, 4]:

Theorem 4.1. *Let $v(s) \in C^4[c,d]$ and $c = s_0 < s_1 < ... < s_{n-1} < s_M = d$ be the partition of $[c,d]$ and $V^*(s)$ be the unique B-spline function that interpolates v. Then there exist constants γ_i independent of h, such that*

$$\|(v - V^*)\|_\infty \leq \gamma_i h^{4-i}, \qquad i = 0, 1, 2, 3.$$

First, we assume the computed B-spline approximation to (2.1) as

$$V^*(s,t) = \sum_{j=-3}^{M-1} D_j^*(t) TB_j^4(s).$$

To estimate the error, $\|v(s,t)-V(s,t)\|_\infty$ we must estimate the errors $\|v(s,t)-V^*(s,t)\|_\infty$ and $\|V^*(s,t)-V(s,t)\|_\infty$ separately. For this purpose, we rewrite the Eq. (2.10) as:

$$v^* - \frac{k\nu^2}{2}(v_{ss})^* = r(s), \tag{4.1}$$

where, $v^* = v_j^n, (v_{ss})^* = (v_{ss})_j^{n+1}$ and $r(s) = v_j^n + \frac{k\nu^2}{2}(v_{ss})_j^n + kg(s_j, t_{n+1})$. Eq. (4.1) can be written in matrix form as:

$$AD = R, \tag{4.2}$$

where, $R = ND^n + h$ and

$$A = \begin{bmatrix} \zeta_1 & \zeta_2 & \zeta_1 & 0 & ... & 0 & 0 \\ q_1 & q_2 & q_1 & 0 & 0 & ... & 0 \\ -\rho_1 & \rho_2 & \rho_3 & \rho_2 & -\rho_1 & ... & 0 \\ \vdots & \vdots & \vdots & \vdots & \vdots & \vdots & \vdots \\ \vdots & \vdots & \vdots & \vdots & \vdots & \vdots & \vdots \\ \vdots & \vdots & \vdots & \vdots & \vdots & \vdots & \vdots \\ 0 & ... & -\rho_1 & \rho_2 & \rho_3 & \rho_2 & -\rho_1 \\ 0 & 0 & \dots & \dots & q_1 & q_2 & q_1 \\ 0 & 0 & \dots & \dots & \zeta_1 & \zeta_2 & \zeta_1 \end{bmatrix}$$

,

$$N = \begin{bmatrix} 0 & 0 & 0 & 0 & ... & 0 & 0 \\ q_3 & q_4 & q_3 & 0 & 0 & ... & 0 \\ \rho_1 & \rho_4 & \rho_5 & \rho_4 & \rho_1 & ... & 0 \\ \vdots & \vdots & \vdots & \vdots & \vdots & \vdots & \vdots \\ \vdots & \vdots & \vdots & \vdots & \vdots & \vdots & \vdots \\ \vdots & \vdots & \vdots & \vdots & \vdots & \vdots & \vdots \\ 0 & ... & \rho_1 & \rho_4 & \rho_5 & \rho_4 & \rho_1 \\ 0 & 0 & \dots & \dots & q_3 & q_4 & q_3 \\ 0 & 0 & \dots & \dots & 0 & 0 & 0 \end{bmatrix},$$

$h = [\alpha(t_{n+1}), kg(s_j, t_{n+1}), ..., kg(s_j, t_{n+1}), \beta(t_{n+1})]^T$, $D^n = [D^n_{-4}, D^n_{-2}, D^n_{-1}, ..., D^n_{M-2}]^T$,
$q_1 = \zeta_1 - \dfrac{k\nu^2\zeta_5}{2}, \quad q_2 = \zeta_2 - \dfrac{k\nu^2\zeta_6}{2}, \quad q_3 = \zeta_1 + \dfrac{k\nu^2\zeta_5}{2}, \quad q_4 = \zeta_2 + \dfrac{k\nu^2\zeta_6}{2}.$
If we replace v^* by V^* in the equation (4.1), then the resulting equation in matrix form becomes

$$AD^* = R^* \tag{4.3}$$

Subtracting (4.3) from (4.2), we obtain

$$A(D^* - D) = (R^* - R). \tag{4.4}$$

Now using (4.1), we have

$$\begin{aligned} |r^*(s_j) - r(s_j)| &= |(v^*(s_j) - v(s_j)) - \frac{k\nu^2}{s}(v^*_{ss}(s_j) - v_{ss}(s_j))| \\ &\le |(v^*(s_j) - v(s_j))| + |\frac{k\nu^2}{2}(v^*_{ss}(s_j) - v_{ss}(s_j))| \end{aligned} \tag{4.5}$$

From (4.5) and theorem (4.1), we have

$$\begin{aligned} \|R^* - R\| &\leq \gamma_0 h^4 + \|\frac{k\nu^2}{2}\|\gamma_2 h^2 \\ &= (\gamma_0 h^2 + \frac{k\nu^2}{2}\gamma_2)h^2 \\ &= M_1 h^2, \end{aligned} \tag{4.6}$$

where $M_1 = \gamma_0 h^2 + \|\frac{k\nu^2}{2}\|\gamma_2$. It is obvious that the matrix A is diagonally dominant and thus nonsingular, so that

$$(D^* - D) = A^{-1}(R^* - R). \tag{4.7}$$

Now using (4.6), we obtain

$$\|D^* - D\| \leq \|A^{-1}\|\|R^* - R\| \leq \|A^{-1}\|(M_1 h^2). \tag{4.8}$$

Let $a_{j,i}$ denote the entries of A and $\eta_j, 0 \leq j \leq M+2$ is the summation of jth row of the matrix A, then we have

$$\eta_0 = \sum_{i=0}^{M+2} a_{0,i} = 2\zeta_1 + \zeta_2,$$

$$\begin{aligned} \eta_1 &= \sum_{i=0}^{M+2} a_{1,i} = 2\zeta_1 + \zeta_2 - k\nu^2\zeta_5 - \frac{k\nu^2\zeta_6}{2}, \\ \eta_j &= \sum_{i=0}^{M+2} a_{j,i} = 2\zeta_1 + \zeta_2 - k\nu^2\omega_1 - \frac{k\nu^2\omega_2}{2} - \frac{k\nu^2\omega_3}{2}, \quad 2 \leq j \leq M \\ \eta_{M+1} &= \sum_{i=0}^{M+2} a_{M+1,i} = 2\zeta_1 + \zeta_2 - k\nu^2\zeta_5 - \frac{k\nu^2\zeta_6}{2}, \\ \eta_{M+2} &= \sum_{i=0}^{M+2} a_{M+2,i} = 2\zeta_1 + \zeta_2. \end{aligned}$$

From the theory of matrices we have,

$$\sum_{j=0}^{M+2} a_{k,j}^{-1}\eta_j = 1, \quad k = 0, 1, ..., M+2, \tag{4.9}$$

where $a_{k,j}^{-1}$ are the elements of A^{-1}. Therefore

$$\|A^{-1}\| = \sum_{j=0}^{M+2} |a_{k,j}^{-1}| \leq \frac{1}{\min \eta_k} = \frac{1}{\xi_l} \leq \frac{1}{|\xi_l|}, \quad 0 \leq k, l \leq M+2. \tag{4.10}$$

Substituting (4.10) into (4.8) we see that

$$\|D^* - D\| \leq \frac{M_1 h^2}{|\xi_l|} = M_2 h^2, \tag{4.11}$$

where $M_2 = \frac{M_1}{|\xi_l|}$ is some finite constant.

Theorem 4.2. *The cubic trigonometric B-splines* $\{TB_{-4}, TB_{-3}, ...TB_M\}$ *defined in relation (2.2) satisfy the inequality*

$$\sum_{j=-3}^{M-1} |TB_j^4(s)| \leq 1.66667, \quad 0 \leq s \leq 1.$$

Proof. Consider,

$$\begin{aligned} |\sum_{j=-3}^{M-1} TB_j^4(s)| &\leq \sum_{j=-3}^{M-1} |TB_j^4(s)| \\ &= |TB_{j-3}^4(s)| + |TB_{j-2}^4(s)| + |TB_{j-1}^4(s)| \\ &= \csc(h)\csc\left(\frac{3h}{2}\right)\sin^2\left(\frac{h}{2}\right) + \frac{2}{1+2\cos(h)} + \csc(h)\csc\left(\frac{3h}{2}\right)\sin^2\left(\frac{h}{2}\right) \\ &\leq 1 \quad \text{for all} \quad h > 0. \end{aligned}$$

Now for $s \in [s_{j+1}, s_{j+2}]$, we have

$$|TB_{j-2}^4(s)| \leq \csc(h)\csc\left(\frac{3h}{2}\right)\sin^2\left(\frac{h}{2}\right),$$

$$|TB_{j-1}^4(s)| \leq \csc(h)\csc\left(\frac{3h}{2}\right)\sin^2\left(\frac{h}{2}\right),$$

$$|TB_{j-3}^4(s)| \leq \frac{2}{1+2\cos(h)},$$

$$|TB_{j-4}^4(s)| \leq \frac{2}{1+2\cos(h)}.$$

Then, we have

$$\sum_{j=-3}^{M-1} |TB_j^4(s)| = |TB_{j-3}^4(s)| + |TB_{j-2}^4(s)| + |TB_{j-1}^4(s)| + |TB_{j-4}^4(s)| \leq 1.66667$$

as required. □

Now, consider

$$V^*(s) - V(s) = \sum_{j=-3}^{M-1} (D_j^* - D_j) TB_j^4(s). \tag{4.12}$$

Using (4.11) and theorem 4.2, we obtain

$$\|V^*(s) - V(s)\| = \left\| \sum_{j=-3}^{M-1} (D_j^* - D_j) TB_j^4(s) \right\| \leq |\sum_{j=-3}^{M-1} TB_j^4(s)| \; \|(D_j^* - D_j)\| \leq 1.66667 M_2 h^2. \tag{4.13}$$

Theorem 4.3. *Let* $v(s)$ *be the exact solution and let* $V(s)$ *be the cubic trigonometric collocation approximation to* $v(s)$ *then the provided scheme has second order convergence in space and*

$$\|v(s) - V(s)\| \leq \omega h^2, \quad \textit{where } \omega = \gamma_0 h^2 + 1.66667 M_2 h^2.$$

Proof. From theorem 4.1, we have

$$\|v(s) - V(s)\| \leq \gamma_0 h^4. \tag{4.14}$$

From (4.13) and (4.14), we obtain

$$\|v(s) - V(s)\| \leq \|v(s) - V^*(s)\| + \|V^*(s) - V(s)\| \leq \gamma_0 h^4 + 1.66667 M_2 h^2 = \omega h^2. \tag{4.15}$$

where $\omega = \gamma_0 h^2 + 1.66667 M_2$. □

5. Numerical experiments and discussion

In this section, some numerical calculations are performed to test the accuracy of the offered scheme. In all examples, we use the following error norm

$$L_\infty = max_j |V_{num}(s_j,t) - v_{exact}(s_j,t)|. \tag{5.1}$$

The numerical order of convergence p is obtained by using the following formula:

$$p = \frac{Log(L_\infty(n)/L_\infty(2n))}{Log(L_\infty(2n)/L_\infty(n))}, \tag{5.2}$$

where $L_\infty(n)$ and $L_\infty(2n)$ are the errors at number of partition n and $2n$ respectively.

Example 1. Consider the heat equation,

$$\frac{\partial v}{\partial t} = \frac{1}{\pi^2}\frac{\partial^2 v}{\partial s^2}, \quad 0 \le s \le 1, \quad t > 0 \tag{5.3}$$

with initial constraint:

$$v(s,0) = \sin(\pi s) \tag{5.4}$$

and the boundary constraints:

$$v(0,t) = 0, \ v(1,t) = 0. \tag{5.5}$$

The analytic solution of the given problem is $v(s,t) = \exp(-t)\sin(\pi s)$. In Table 1, the comparative analysis of absolute errors are given with those of [9]. Figure 1 demonstrates the behavior of exact and numerical solutions at various time stages. On the other hand Figure 2 illustrates the graphical representation of absolute errors in 2D and 3D. Figure 3 shows the rattling accuracy that exists between the exact and approximate solutions.

The approximate solution when $t = 1, k = 0.01$ and $M = 20$ is given by

$$V(s,1) = \begin{cases} -0.000277763\cos(\frac{s}{2}) + 0.000277763\cos^3(\frac{s}{2}) - & \\ 3.69641\sin^3(\frac{s}{2}) + \sin(\frac{s}{2})(-8.77708 - 0.000416645\sin(s)) + & \\ 2.77231\csc(\frac{s}{2})\sin^2(s), & s \in [0, \frac{1}{20}] \\ -0.00510497\cos(\frac{s}{2}) + 0.00510095\cos^3(\frac{s}{2}) - & \\ 3.63222\sin^3(\frac{s}{2}) + \sin(\frac{s}{2})(-8.58403 - 0.00765142\sin(s)) + & \\ 2.72417\csc(\frac{s}{2})\sin^2(s), & s \in [\frac{1}{20}, \frac{1}{10}] \\ & \\ -0.0261732\cos(\frac{s}{2}) + 0.026099\cos^3(\frac{s}{2}) - 3.49329\sin^3(\frac{s}{2}) + & \\ \sin(\frac{s}{2})(-8.16302 - 0.0391486\sin(s)) + 2.61997\csc(\frac{s}{2})\sin^2(s), & s \in [\frac{1}{10}, \frac{3}{20}] \\ \vdots & \\ \vdots & \\ -3.93653\cos(\frac{s}{2}) + 3.48638\cos^3(\frac{s}{2}) + 0.221072\sin^3(\frac{s}{2}) + & \\ \sin(\frac{s}{2})(7.15117 - 5.22958\sin(s)) - 0.165804\csc(\frac{s}{2})\sin^2(s), & s \in [\frac{17}{20}, \frac{9}{10}] \\ -4.11988\cos(\frac{s}{2}) + 3.62349\cos^3(\frac{s}{2}) + 0.251845\sin^3(\frac{s}{2}) + & \\ \sin(\frac{s}{2})(7.53075 - 5.43523\sin(s)) - 0.188884\csc(\frac{s}{2})\sin^2(s), & s \in [\frac{9}{10}, \frac{19}{20}] \\ -4.2082\cos(\frac{s}{2}) + 3.68717\cos^3(\frac{s}{2}) + 0.261197\sin^3(\frac{s}{2}) + & \\ \sin(\frac{s}{2})(7.70248 - 5.53076\sin(s)) - 0.195898\csc(\frac{s}{2})\sin^2(s), & s \in [\frac{19}{20}, 1]. \end{cases}$$

Table 1: Comparison of absolute errors when $k = 0.01$ at $T = 2$ for example 1.

s	$M = 16$		$M = 20$	
	Present scheme	CuBS[9]	Present scheme	CuBS[9]
0.1	3.95199×10^{-5}	2.69092×10^{-4}	2.51528×10^{-5}	1.72467×10^{-4}
0.2	7.53284×10^{-5}	5.11635×10^{-4}	4.78434×10^{-5}	3.28052×10^{-4}
0.3	1.03726×10^{-4}	7.04146×10^{-4}	6.58508×10^{-5}	4.51526×10^{-4}
0.4	1.21722×10^{-4}	8.28057×10^{-4}	7.74123×10^{-5}	5.30800×10^{-4}
0.5	1.28357×10^{-4}	8.70181×10^{-4}	8.13961×10^{-5}	5.58116×10^{-4}
0.6	1.21722×10^{-4}	8.28057×10^{-4}	7.74123×10^{-5}	5.30800×10^{-4}
0.7	1.03726×10^{-4}	7.04146×10^{-4}	6.58508×10^{-5}	4.51526×10^{-4}
0.8	7.53284×10^{-5}	5.11635×10^{-4}	4.78434×10^{-5}	3.28052×10^{-4}
0.9	3.95199×10^{-5}	2.69092×10^{-4}	2.51528×10^{-5}	1.72467×10^{-4}

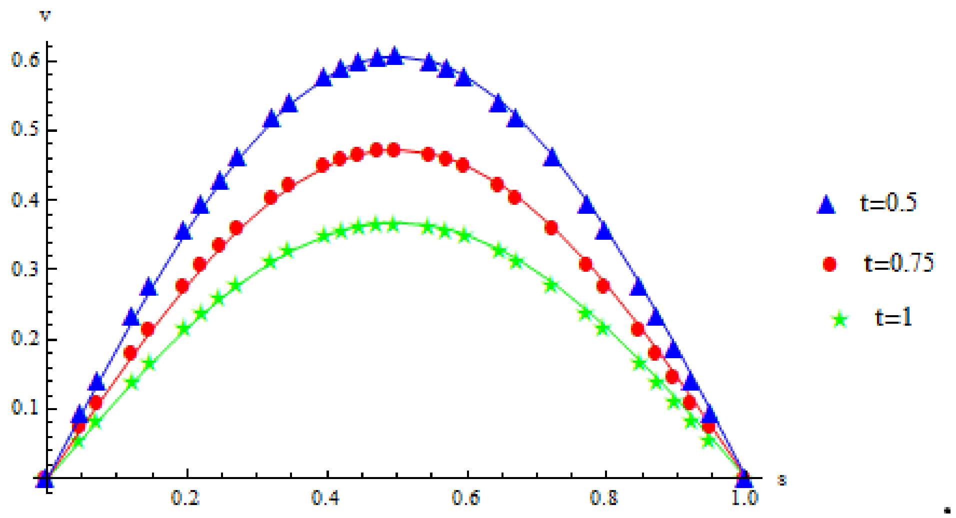

Figure 1: The approximate (stars, circles, triangles) and exact (solid lines) solutions for various time stages when $M = 80, k = 0.01$ for example 1.

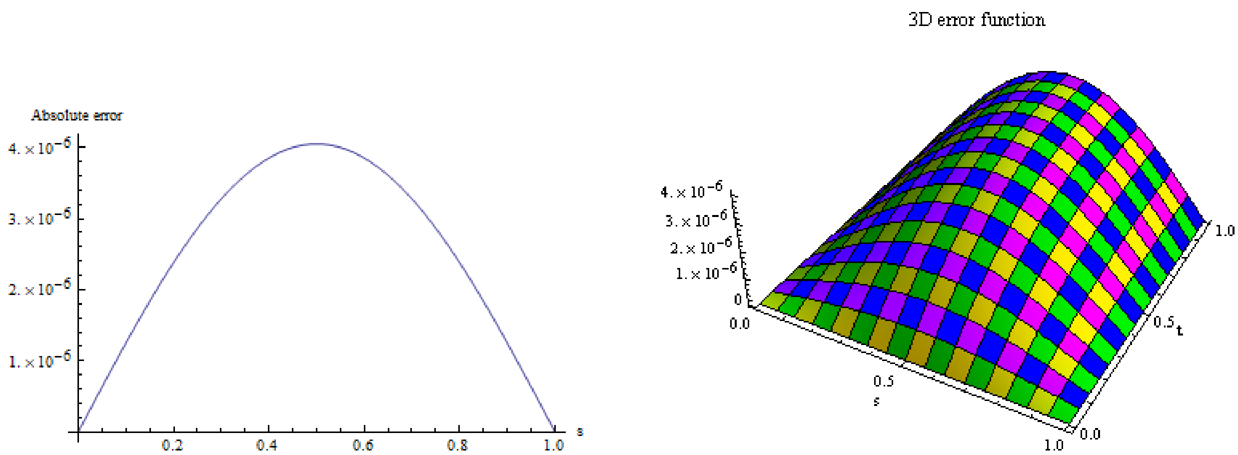

Figure 2: 2D and 3D error profiles when $M = 80, k = 0.01, T = 1$ for example 1.

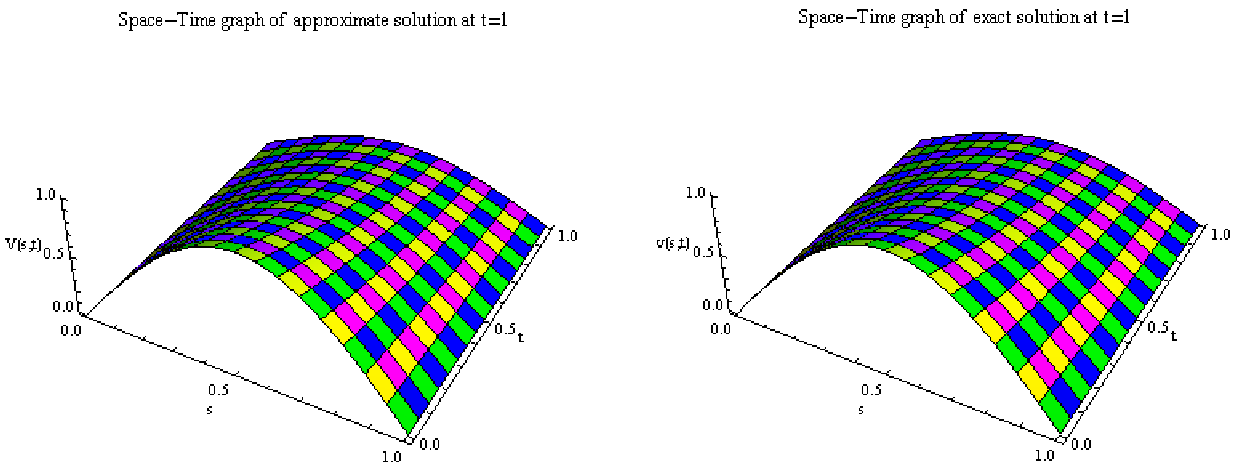

Figure 3: Comparison of exact and approximate solutions with $T = 1, M = 80, k = 0.01$ for example 1.

Example 2. Consider the heat equation,

$$\frac{\partial v}{\partial t} = \frac{\partial^2 v}{\partial s^2}, \quad 0 \leq s \leq 1 \quad , t > 0 \tag{5.6}$$

with initial constraint:

$$v(s, 0) = \sin(\pi s) \tag{5.7}$$

and the boundary constraints:

$$v(0, t) = 0,\ v(1, t) = 0. \tag{5.8}$$

The analytic solution is $v(s, t) = \exp(-\pi^2 t)\sin(\pi s)$. By employing the present scheme on example 2 the values of absolute errors are derived out in Table 2. The comparison sheds light on the fact that presented scheme gives much accuracy. In Figure 4, the exact and approximate solutions are shown at various time stages. Figure 5 depicts the 2D and 3D absolute error profiles at $T = 1$. A 3D contrast between exact and numerical solutions is shown in Figure 6 and the results are very well. The approximate solution when $t = 1, k = 0.01$ and $M = 20$ is given by

$$V(s,1) = \begin{cases} -0.0002778\cos(\frac{s}{2}) + 0.0002778\cos^3(\frac{s}{2}) + 0.0041726\sin^3(\frac{s}{2}) + \\ \sin(\frac{s}{2})(0.0128571 - 0.0004166\sin(s)) - 0.0031294\csc(\frac{s}{2})\sin^2(s), & s \in [0, \frac{1}{20}] \\ 0.0001681\cos(\frac{s}{2}) - 0.0001677\cos^3(\frac{s}{2}) - 0.0017559\sin^3(\frac{s}{2}) + \\ \sin(\frac{s}{2})(-0.0049729 + 0.0002516\sin(s)) + 0.0013169\csc(\frac{s}{2})\sin^2(s), & s \in [\frac{1}{20}, \frac{1}{10}] \\ -0.0000742\cos(\frac{s}{2}) + 0.0000737\cos^3(\frac{s}{2}) - 0.0001584\sin^3(\frac{s}{2}) + \\ \sin(\frac{s}{2})(-0.0001320 - 0.0001106\sin(s)) + 0.0001188\csc(\frac{s}{2})\sin^2(s), & s \in [\frac{1}{10}, \frac{3}{20}] \\ \vdots \\ \vdots \\ -0.0001284\cos(\frac{s}{2}) + 0.0001632\cos(\frac{s}{2})^3 - 0.0000623\sin^3(\frac{s}{2}) + \\ \sin(\frac{s}{2})(0.0000802 - 0.0002448\sin(s)) + 0.0000468\csc(\frac{s}{2})\sin^2(s), & s \in [\frac{17}{20}, \frac{9}{10}] \\ -0.0022366\cos(\frac{s}{2}) + 0.0017396\cos^3(\frac{s}{2}) + 0.0002915\sin^3(\frac{s}{2}) + \\ \sin(\frac{s}{2})(0.0044447 - 0.0026095\sin(s)) - 0.0002186\csc(\frac{s}{2})\sin^2(s), & s \in [\frac{9}{10}, \frac{19}{20}] \\ 0.00592028\cos(\frac{s}{2}) - 0.0041425\cos^3(\frac{s}{2}) - 0.0005722\sin^3(\frac{s}{2}) + \\ \sin(\frac{s}{2})(-0.0114164 + 0.0062137\sin(s)) + 0.0004292\csc(\frac{s}{2})\sin^2(s), & s \in [\frac{19}{20}, 1]. \end{cases}$$

Table 2: Comparison of absolute errors for example 2 at $T = 1$.

$h = k$	CuBS[10]	Present scheme	p
$\frac{1}{5}$	1.4145×10^{-1}	4.9192×10^{-5}	0.65401
$\frac{1}{10}$	3.7195×10^{-2}	3.1262×10^{-5}	1.70720
$\frac{1}{20}$	8.4588×10^{-3}	9.5741×10^{-6}	1.93105
$\frac{1}{40}$	2.0698×10^{-3}	2.5107×10^{-6}	1.98299
$\frac{1}{80}$	5.1473×10^{-4}	6.3512×10^{-7}	

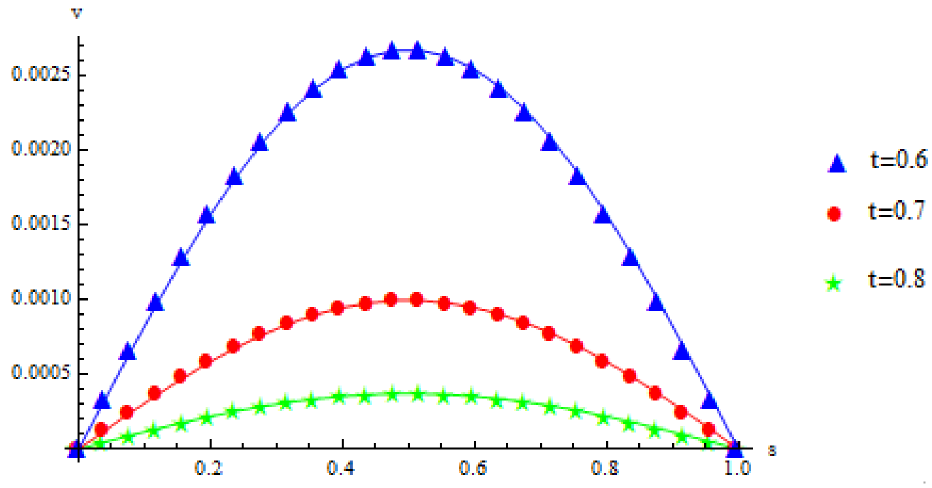

Figure 4: The approximate (stars, circles, triangles) and exact (solid lines) solutions for various time stages when $M = 50, k = 0.01$ for example 2.

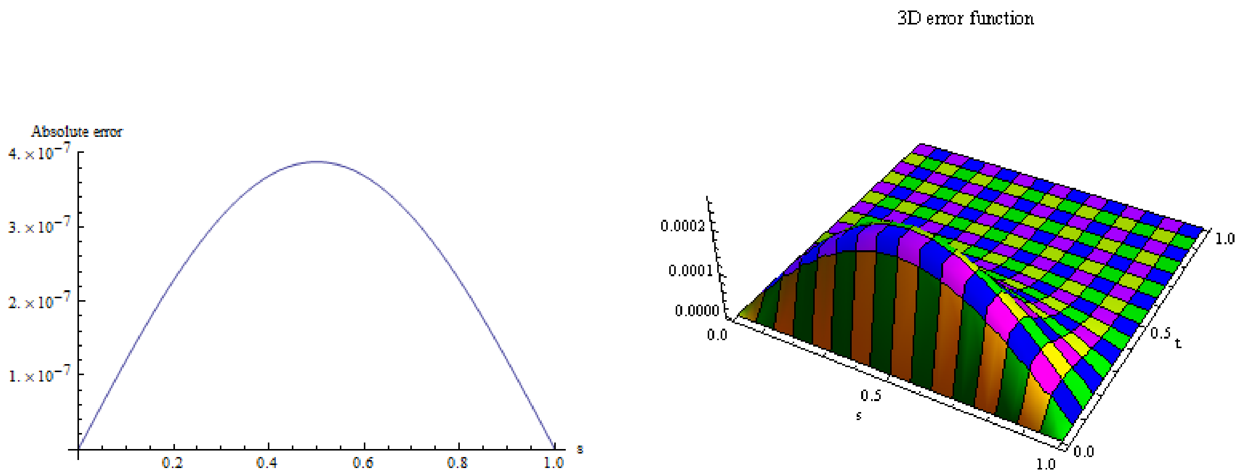

Figure 5: 2D and 3D error profiles when $M = 50, k = 0.01, T = 1$ for example 2.

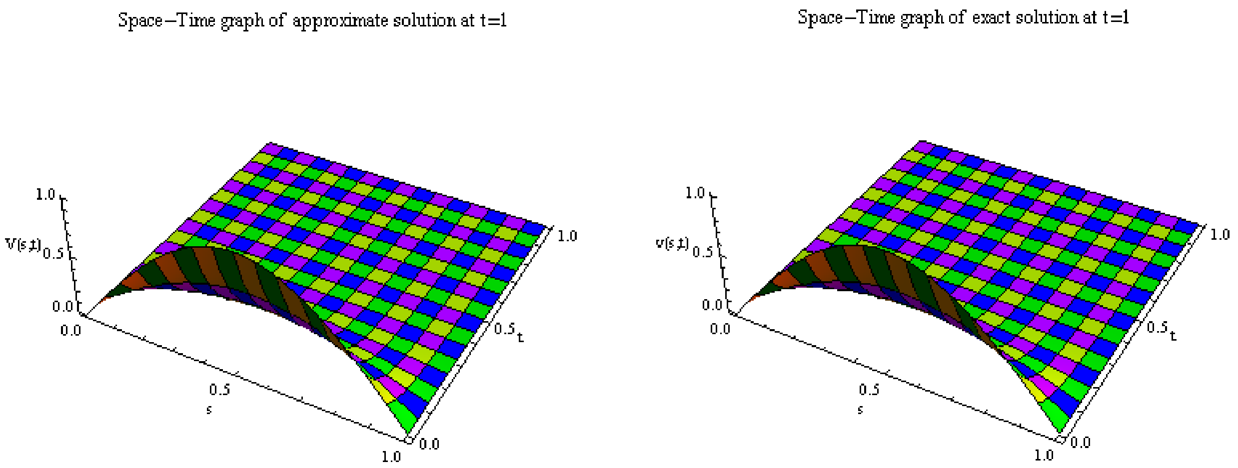

Figure 6: Comparison of exact and approximate solutions with $T = 1, M = 50, k = 0.01$ for example 2.

Example 3. Consider the heat equation,

$$\frac{\partial v}{\partial t} = \frac{\partial^2 v}{\partial s^2}, \quad 0 \le s \le 1, \quad t > 0 \tag{5.9}$$

with initial constraint:

$$v(s, 0) = \cos(\frac{\pi s}{2}) \tag{5.10}$$

and the boundary constraints:

$$v(0, t) = \exp(\frac{\pi^2 t}{4}), \; v(1, t) = 0. \tag{5.11}$$

The analytic solution is $v(s, t) = \exp(\frac{-\pi^2 t}{4}) \cos(\frac{\pi s}{2})$. To achieve numerical results on the above-mentioned problem the presented scheme is utilized. Table 3 discusses the comparison that exists between the absolute errors that are derived out by the present method and by the method of [11]. Figure 7 deals with the behavior of exact and approximate solutions at various time stages. All the graphs are in excellent affirmation. 2D and 3D error profiles are shown in Figure 8 at $T = 1$. A 3D contrast between the exact and numerical solutions is figured out in Figure 9. The approximate solution when $t = 1, k = 0.01$ and $M = 20$ is given by

$$V(s,1) = \begin{cases} -0.00932586\cos(\frac{s}{2}) + 0.0941308\cos^3(\frac{s}{2}) + 0.00217188\sin^3(\frac{s}{2}) + \\ \sin(\frac{s}{2})(0.00651287 - 0.141196\sin(s)) - 0.00162891\csc(\frac{s}{2})\sin^2(s), & s \in [0, \frac{1}{20}] \\ -0.0095084\cos(\frac{s}{2}) + 0.094312\cos^3(\frac{s}{2}) + 0.00229618\sin^3(\frac{s}{2}) + \\ \sin(\frac{s}{2})(0.00694553 - 0.141468\sin(s)) - 0.00172214\csc(\frac{s}{2})\sin^2(s), & s \in [\frac{1}{20}, \frac{1}{10}] \\ -0.00971627\cos(\frac{s}{2}) + 0.0945171\cos^3(\frac{s}{2}) + 0.00295925\sin^3(\frac{s}{2}) + \\ \sin(\frac{s}{2})(0.00901732 - 0.141776\sin(s)) - 0.00221944\csc(\frac{s}{2})\sin^2(s), & s \in [\frac{1}{10}, \frac{3}{20}] \\ \vdots \\ -0.0136572\cos(\frac{s}{2}) + 0.0980453\cos^3(\frac{s}{2}) + 0.00693266\sin^3(\frac{s}{2}) + \\ \sin(\frac{s}{2})(0.0249572 - 0.147068\sin(s)) - 0.0051995\csc(\frac{s}{2})\sin^2(s), & s \in [\frac{17}{20}, \frac{9}{10}] \\ -0.0138031\cos(\frac{s}{2}) + 0.0981544\cos^3(\frac{s}{2}) + 0.00695714\sin^3(\frac{s}{2}) + \\ \sin(\frac{s}{2})(0.0252591 - 0.147232\sin(s)) - 0.00521786\csc(\frac{s}{2})\sin^2(s), & s \in [\frac{9}{10}, \frac{19}{20}] \\ -0.0138496\cos(\frac{s}{2}) + 0.0981879\cos^3(\frac{s}{2}) + 0.00696207\sin^3(\frac{s}{2}) + \\ \sin(\frac{s}{2})(0.0253495 - 0.147282\sin(s)) - 0.00522155\csc(\frac{s}{2})\sin^2(s), & s \in [\frac{19}{20}, 1]. \end{cases}$$

Table 3: Absolute errors and numerical results for $h = k = 0.05$ for example 3 at $T = 1$.

s	Exact	Present scheme	CuBS[11]	Present Scheme	CuBS[11]
0.1	0.0837609	0.0837490	0.0827029	1.188×10^{-5}	1.058×10^{-3}
0.2	0.0806543	0.0806336	0.0795990	2.072×10^{-5}	1.055×10^{-3}
0.3	0.0755618	0.0755352	0.0745108	2.658×10^{-5}	1.051×10^{-3}
0.4	0.0686087	0.0685791	0.0675632	2.956×10^{-5}	1.045×10^{-3}
0.5	0.0599662	0.0599366	0.0589270	2.957×10^{-5}	1.039×10^{-3}
0.6	0.0498471	0.0498200	0.0488146	2.711×10^{-5}	1.033×10^{-3}
0.7	0.0385007	0.0384783	0.0374744	2.235×10^{-5}	1.026×10^{-3}
0.8	0.0262062	0.0261903	0.0251852	1.588×10^{-5}	1.021×10^{-3}
0.9	0.0132664	0.0132582	0.0122492	8.220×10^{-6}	1.017×10^{-3}

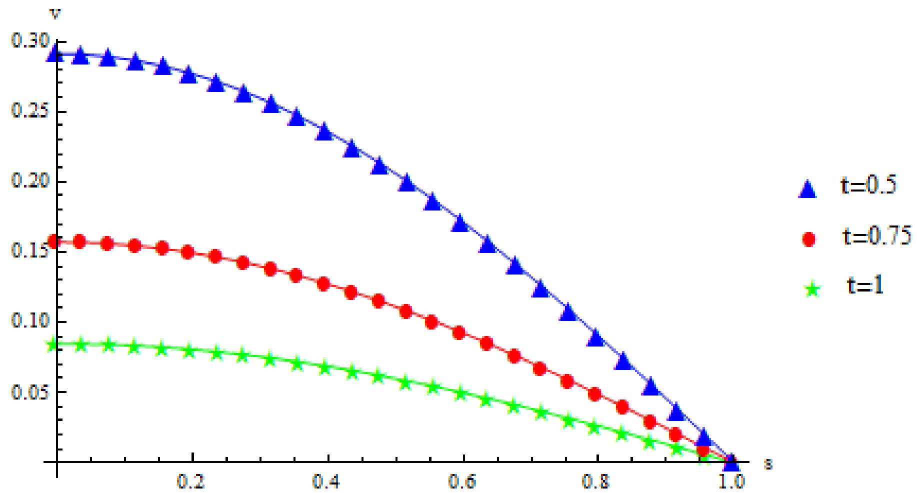

Figure 7: The approximate (stars, circles, triangles) and exact (solid lines) solutions for various time stages when $M = 50, k = 0.01$ for example 3.

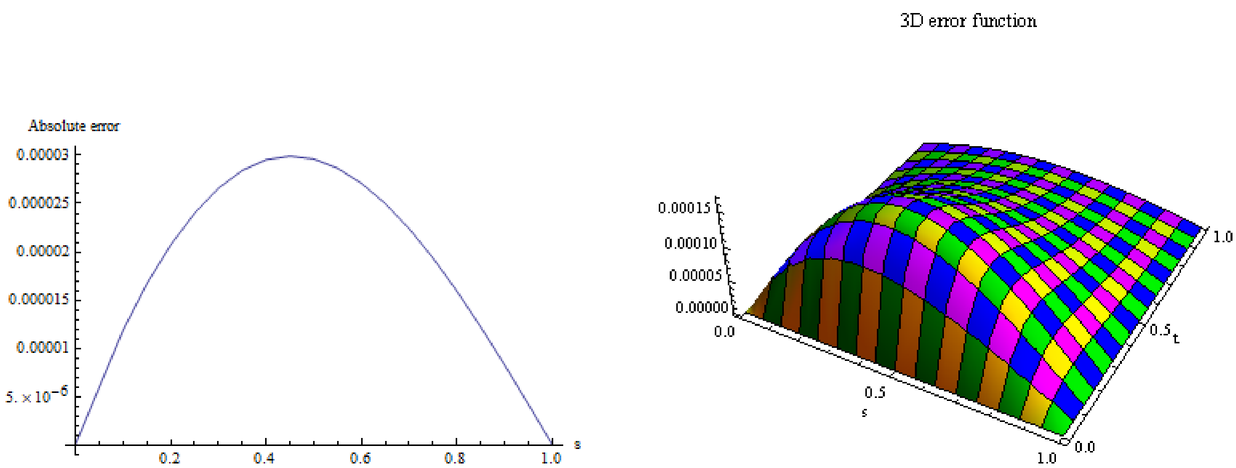

Figure 8: 2D and 3D error profiles when $M = 20, k = 0.05, T = 1$ for example 3.

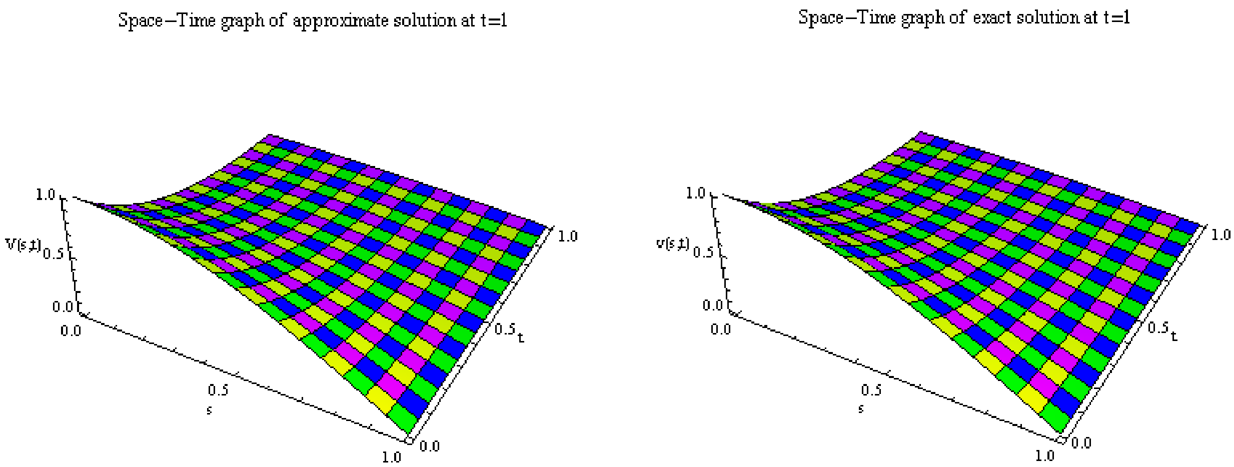

Figure 9: Comparison of exact and approximate solutions with $T = 1, M = 20, k = 0.05$ for example 3.

Example 4. Consider the heat equation,

$$\frac{\partial v}{\partial t} = \frac{\partial^2 v}{\partial s^2} - \exp(-\sin t - s)(\cos t + 1), \quad 0 \leq s \leq 1, \quad t > 0 \tag{5.12}$$

with initial constraint:

$$v(s, 0) = \exp(-s) \tag{5.13}$$

and the non-classical boundary constraints:

$$\begin{cases} v(0,t) = \int_0^1 \frac{e}{e-2} s\, v(s,t) ds, \\ v(1,t) = \int_0^1 \frac{2}{e+\sin 1 - \cos 1} \cos s v(s,t) ds, \end{cases} \qquad t > 0. \tag{5.14}$$

The analytic solution of the given problem is $v(s,t) = \exp(-s - sint)$. By utilizing the proposed scheme the numerical results are acquired. An excellent comparison between absolute errors computed by our scheme and the scheme of [22] is discussed in Table 4. At different time stages a close comparison between the exact and numerical solutions is depicted in Figure 10. Figure 11 plots 2D and 3D absolute errors at $T = 1$. Figure 12 deals with the 3D comparison that occurs between the exact and numerical solutions. The approximate solution when $t = 1, k = 0.01$ and $M = 20$ is given by

$$V(s,1) = \begin{cases} 0.703278 \cos(\frac{s}{2}) - 0.272202 \cos^3(\frac{s}{2}) - 0.245111 \sin^3(\frac{s}{2}) + \\ \sin(\frac{s}{2})(-1.59479 + 0.408303 \sin(s)) + 0.183834 \csc(\frac{s}{2}) \sin^2(s), & s \in [0, \frac{1}{20}] \\ 0.693563 \cos(\frac{s}{2}) - 0.262495 \cos^3(\frac{s}{2}) - 0.115922 \sin^3(\frac{s}{2}) + \\ \sin(\frac{s}{2})(-1.20625 + 0.393742 \sin(s)) + 0.0869418 \csc(\frac{s}{2}) \sin^2(s), & s \in [\frac{1}{20}, \frac{1}{10}] \\ 0.69364 \cos(\frac{s}{2}) - 0.262572 \cos^3(\frac{s}{2}) - 0.116433 \sin^3(\frac{s}{2}) + \\ \sin(\frac{s}{2})(-1.2078 + 0.393858 \sin(s)) + 0.087325 \csc(\frac{s}{2}) \sin^2(s), & s \in [\frac{1}{10}, \frac{3}{20}] \\ \vdots \\ 0.508474 \cos(\frac{s}{2}) - 0.0980879 \cos^3(\frac{s}{2}) + 0.0894798 \sin^3(\frac{s}{2}) + \\ \sin(\frac{s}{2})(-0.399339 + 0.147132 \sin(s)) - 0.0671099 \csc(\frac{s}{2}) \sin^2(s), & s \in [\frac{17}{20}, \frac{9}{10}] \\ 0.505903 \cos(\frac{s}{2}) - 0.0961654 \cos^3(\frac{s}{2}) + 0.0899113 \sin^3(\frac{s}{2}) + \\ \sin(\frac{s}{2})(-0.394017 + 0.144248 \sin(s)) - 0.0674335 \csc(\frac{s}{2}) \sin^2(s), & s \in [\frac{9}{10}, \frac{19}{20}] \\ 0.439152 \cos(\frac{s}{2}) - 0.04803 \cos^3(\frac{s}{2}) + 0.0969795 \sin^3(\frac{s}{2}) + \\ \sin(\frac{s}{2})(-0.26422 + 0.0720451 \sin(s)) - 0.0727346 \csc(\frac{s}{2}) \sin^2(s), & s \in [\frac{19}{20}, 1]. \end{cases}$$

Table 4: Comparison of absolute errors when $h = 0.05$ at varied time stages for example 4.

t	$k = 0.01$		$k = 0.005$	
	TMOL[22]	Present scheme	TMOL[22]	Present scheme
0.1	4.50×10^{-4}	4.77×10^{-4}	4.00×10^{-5}	2.42×10^{-4}
0.3	1.40×10^{-3}	6.49×10^{-4}	1.40×10^{-4}	3.30×10^{-4}
0.5	2.50×10^{-3}	5.74×10^{-4}	2.50×10^{-4}	2.91×10^{-4}
0.7	4.00×10^{-3}	4.68×10^{-4}	4.00×10^{-4}	2.38×10^{-4}
0.9	5.50×10^{-3}	3.71×10^{-4}	5.50×10^{-4}	1.89×10^{-4}
1.0	6.00×10^{-4}	3.28×10^{-4}	6.00×10^{-4}	1.67×10^{-4}

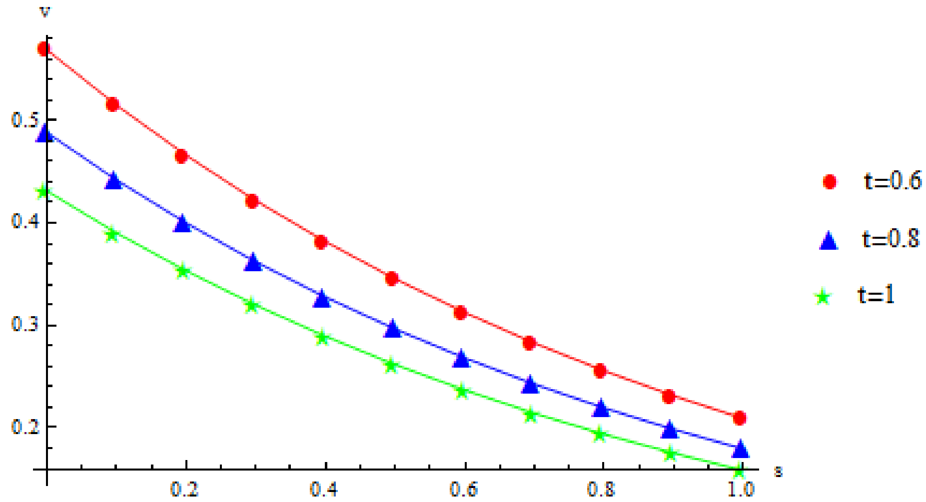

Figure 10: The approximate (stars, circles, triangles) and exact (solid lines) solutions for various time stages when $M = 20, k = 0.01$ for example 4.

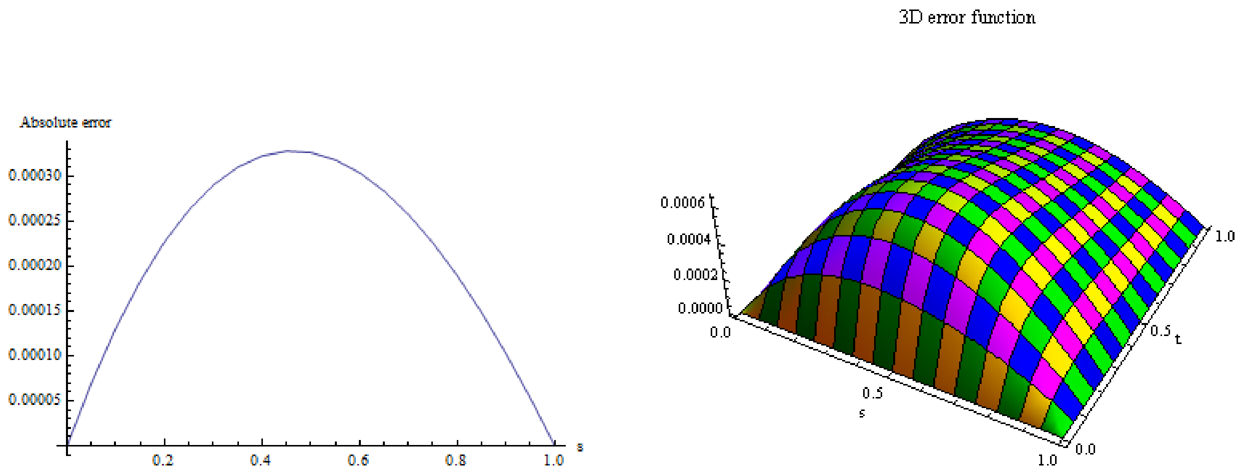

Figure 11: 2D and 3D error profiles when $M = 20, k = 0.01, T = 1$ for example 4.

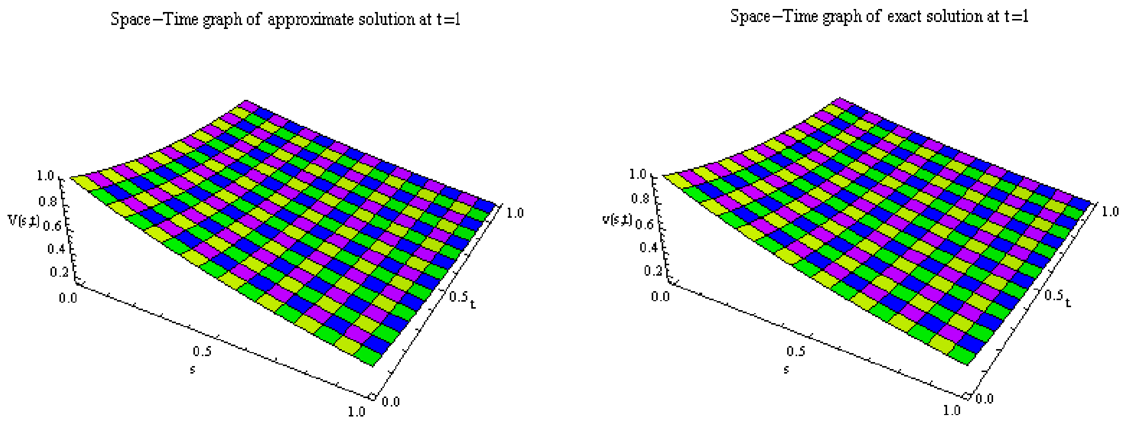

Figure 12: Comparison of exact and numerical solutions with $T = 1, M = 20, k = 0.01$ for example 4.

Example 5. Consider the heat equation,

$$\frac{\partial v}{\partial t} = \frac{\partial^2 v}{\partial s^2} + (\pi^2 - 1)\exp(-t)(\sin \pi s + \cos \pi s), \quad 0 \le s \le 1, \quad t > 0 \tag{5.15}$$

with initial constraint:

$$v(s, 0) = (\sin \pi s + \cos \pi s) \tag{5.16}$$

and the non-classical boundary constraints:

$$\begin{cases} v(0,t) = \int_0^1 2\sin(\pi s)v(s,t)ds, \\ v(1,t) = \int_0^1 -2\cos(\pi s)v(s,t)ds, \end{cases} \qquad t > 0. \tag{5.17}$$

The analytic solution of the given problem is $v(s,t) = \exp(-t)(\sin \pi s + \cos \pi s)$. To achieve the desired numerical results the presented scheme is applied in example 5. The absolute errors are being compared with those of obtained in [2] at various time stages in Table 5. On the other hand, Figure 13 clearly demonstrates the comparison that exist between exact and numerical solutions at various time stages. All the graphs are also agree with the said data. Figure 14 depicts the 2D and 3D error profiles at $T = 1$. A 3D comparison between the exact and numerical solutions is presented to exhibit the exactness of the scheme in Figure 15.

The approximate solution when $t = 1, k = 0.01$ and $M = 20$ is given by

$$V(s,1) = \begin{cases} -1.42349\cos(\frac{s}{2}) + 1.79137\cos^3(\frac{s}{2}) - 3.00046\sin^3(\frac{s}{2}) + \\ \sin(\frac{s}{2})(-6.70549 - 2.68705\sin(s)) + 2.25034\csc(\frac{s}{2})\sin^2(s), & s \in [0, \frac{1}{20}] \\ -1.5271\cos(\frac{s}{2}) + 1.89462\cos^3(\frac{s}{2}) - 2.35572\sin^3(\frac{s}{2}) + \\ \sin(\frac{s}{2})(-4.75 - 2.84193\sin(s)) + 1.76679\csc(\frac{s}{2})\sin^2(s), & s \in [\frac{1}{20}, \frac{1}{10}] \\ -1.65212\cos(\frac{s}{2}) + 2.01871\cos^3(\frac{s}{2}) - 1.81356\sin^3(\frac{s}{2}) + \\ \sin(\frac{s}{2})(-3.08615 - 3.02806\sin(s)) + 1.36017\csc(\frac{s}{2})\sin^2(s), & s \in [\frac{1}{10}, \frac{3}{20}] \\ \vdots \\ -4.40323\cos(\frac{s}{2}) + 4.59869\cos^3(\frac{s}{2}) + 2.20717\sin^3(\frac{s}{2}) + \\ \sin(\frac{s}{2})(11.2074 - 6.89803\sin(s)) - 1.65538\csc(\frac{s}{2})\sin^2(s), & s \in [\frac{17}{20}, \frac{9}{10}] \\ -4.2166\cos(\frac{s}{2}) + 4.45436\cos^3(\frac{s}{2}) + 2.16319\sin^3(\frac{s}{2}) + \\ \sin(\frac{s}{2})(10.7951 - 6.68155\sin(s)) - 1.62239\csc(\frac{s}{2})\sin^2(s), & s \in [\frac{9}{10}, \frac{19}{20}] \\ -3.9106\cos(\frac{s}{2}) + 4.21808\cos^3(\frac{s}{2}) + 2.09443\sin^3(\frac{s}{2}) + \\ \sin(\frac{s}{2})(10.1263 - 6.32713\sin(s)) - 1.57082\csc(\frac{s}{2})\sin^2(s), & s \in [\frac{19}{20}, 1]. \end{cases}$$

Table 5: Comparison of absolute errors when $h = 0.01$ at various time stages for example 5.

t	$k = 0.01$		$k = 0.001$	
	CuTBS[2]	Present scheme	CuTBS[2]	Present scheme
0.1	3.05×10^{-3}	2.99×10^{-3}	3.42×10^{-4}	2.92×10^{-4}
0.3	3.70×10^{-3}	3.64×10^{-3}	4.15×10^{-4}	3.55×10^{-4}
0.5	3.20×10^{-3}	3.15×10^{-3}	3.59×10^{-4}	3.07×10^{-4}
0.7	2.64×10^{-3}	2.60×10^{-3}	2.97×10^{-4}	2.54×10^{-4}
0.9	2.17×10^{-3}	2.13×10^{-3}	2.43×10^{-4}	2.08×10^{-4}
1.0	1.96×10^{-3}	1.93×10^{-3}	2.20×10^{-4}	1.88×10^{-4}

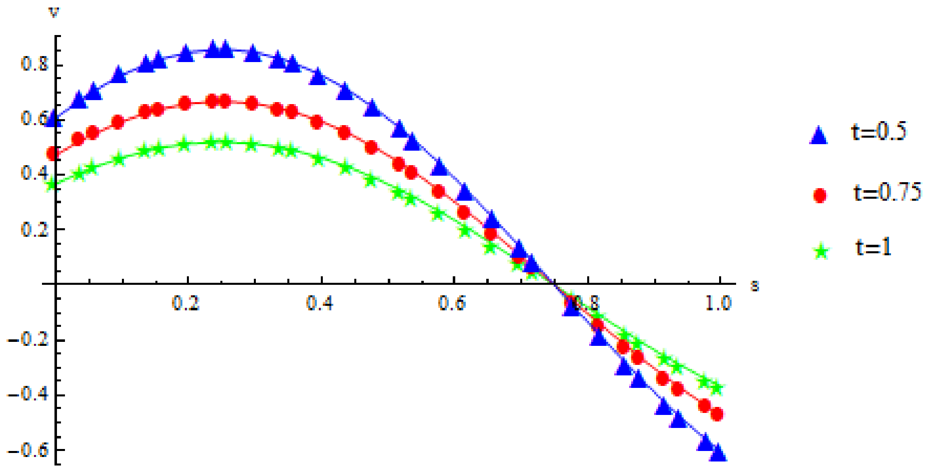

Figure 13: The approximate (stars, circles, triangles) and exact (solid lines) solutions for various time stages when $M = 100, k = 0.01$ for example 5.

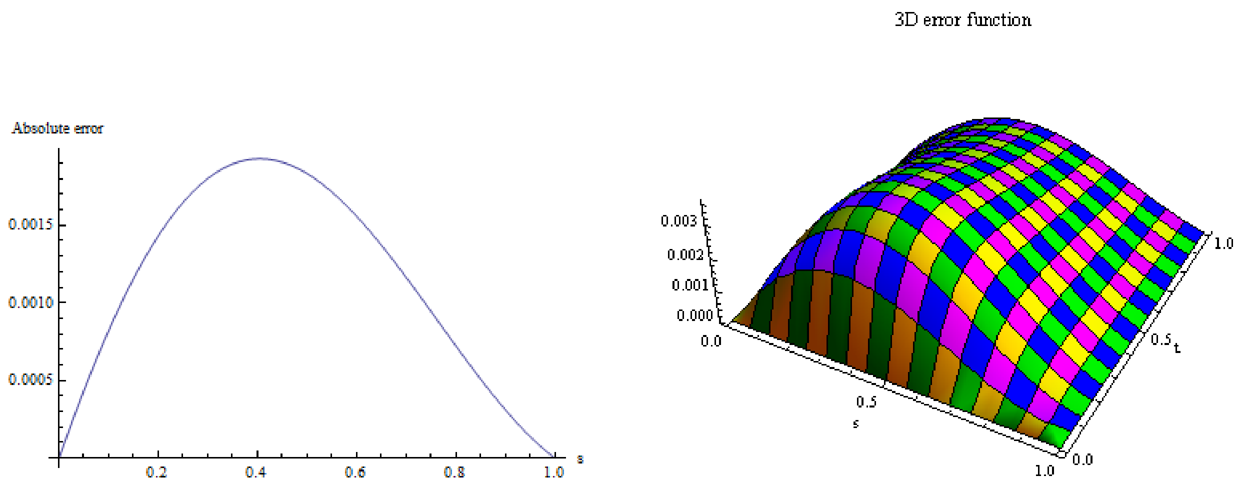

Figure 14: 2D and 3D error profile when $M = 100, k = 0.01, T = 1$ for example 5.

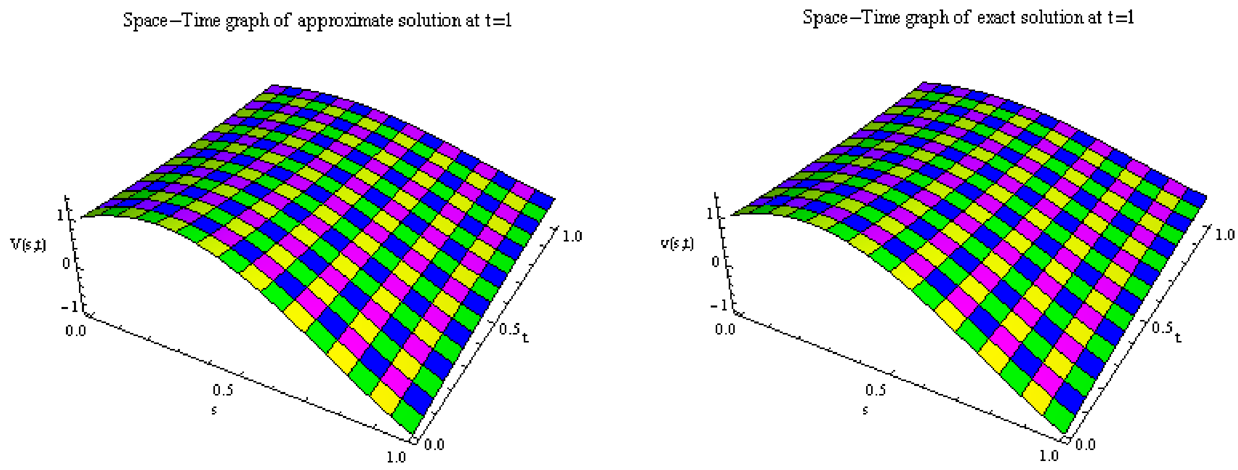

Figure 15: Comparison of exact and numerical solutions with $T = 1, M = 100, k = 0.01$ for example 5.

6. Concluding Remarks

In this study Hermite formula is used for the approximation of second-order derivatives in cubic trigonometric B-spline collocation method to obtain the approximate solution of the heat equation. The smooth piecewise cubic trigonometric B-splines have been used to approximate derivatives in space whereas a standard finite difference has been used to discretize the time derivative. The Hermite formula has been utilized in this technique to refine the scheme. A stability analysis of the scheme is additionally given to confirm that the errors do not expatiate. The numerical solution is obtained as a piecewise smooth function enabling one to find approximation at any desired location in the domain. The scheme's precision is illustrated by comparing the numerical results with those published in literature. Numerical and graphical comparisons show that the given scheme is better and very proficient in computational terms.

Acknowledgements:

The authors are grateful to anonymous referees for their valuable suggestions which significantly improved this manuscript.

References

[1] Abbas, M., Majid, A. A., Ismail, A. I. M., & Rashid, A. (2014). The application of cubic trigonometric B-spline to the numerical solution of the hyperbolic problems. *Applied Mathematics and Computation, 239*, 74-88. 2, 2

[2] Abbas, M., Majid, A. A., Ismail, A. I. M., & Rashid, A. (2014, January). Numerical method using cubic trigonometric B-spline technique for nonclassical diffusion problems. In *Abstract and applied analysis* (Vol. 2014). Hindawi. 1, 5, 5

[3] Al-Said, E. A. (2001). The use of cubic splines in the numerical solution of a system of second-order boundary value problems. *Computers & Mathematics with Applications, 42*(6-7), 861-869. 1

[4] de Boor, C. (1968). On the convergence of odd-degree spline interpolation. *Journal of approximation theory, 1*(4), 452-463. 4

[5] aglar, H., zer, M., & aglar, N. (2008). The numerical solution of the one-dimensional heat equation by using third degree B-spline functions. *Chaos, Solitons & Fractals, 38*(4), 1197-1201. 1

[6] Cahlon, B., Kulkarni, D. M., & Shi, P. (1995). Stepwise stability for the heat equation with a nonlocal constraint. *SIAM journal on numerical analysis, 32*(2), 571-593. 1

[7] Dehghan, M. (2005). Efficient techniques for the second-order parabolic equation subject to nonlocal specifications. *Applied Numerical Mathematics, 52*(1), 39-62. 1

[8] Dehghan, M. (2006). A computational study of the one-dimensional parabolic equation subject to nonclassical boundary specifications. *Numerical Methods for Partial Differential Equations: An International Journal, 22*(1), 220-257. 1

[9] Goh, J., Majid, A. A., & Ismail, A. I. M. (2011). Numerical method using cubic B-spline for the heat and wave equation. *Computers & Mathematics with Applications, 62*(12), 4492-4498. 1, 5, 1

[10] Goh, J., & Ismail, A. I. M. (2012). Cubic B-spline collocation method for one-dimensional heat and advection-diffusion equations. *Journal of Applied Mathematics, 2012*. 1, 2

[11] Goh, J., Majid, A. A., & Ismail, A. I. M. (2010, October). A comparison of some splines-based methods for the one-dimensional heat equation. In *Proceedings of World Academy of Science, Engineering and Technology* (Vol. 70, pp. 858-861). 1, 5, 3

[12] Golbabai, A., & Javidi, M. (2007). A numerical solution for non-classical parabolic problem based on Chebyshev spectral collocation method. *Applied mathematics and computation, 190*(1), 179-185. 1

[13] Gorguis, A., & Chan, W. K. B. (2008). Heat equation and its comparative solutions. *Computers & Mathematics with Applications, 55*(12), 2973-2980. 1

[14] Jator, S., & Sinkala, Z. (2007). A high order B-spline collocation method for linear boundary value problems. *Applied Mathematics and Computation, 191*(1), 100-116.

[15] Hall, C. A. (1968). On error bounds for spline interpolation. *Journal of approximation theory, 1*(2), 209-218. 1

[16] Khabir, M. H., & Farah, R. A. (2017). Cubic B-spline collocation method for one-dimensional heat equation. *Pure and Applied Mathematics Journal, 6*(1), 51-58. 4

[17] Khader, M. M., & Adel, M. H. (2016). Numerical solutions of fractional wave equations using an efficient class of FDM based on the Hermite formula. *Advances in Difference Equations, 2016*(1), 1-10. 1

[18] Kumar, M., & Gupta, Y. (2010). Methods for solving singular boundary value problems using splines: a review. *Journal of Applied Mathematics and Computing, 32*(1), 265-278. 2

[19] Mohebbi, A., & Dehghan, M. (2010). High-order compact solution of the one-dimensional heat and advectiondiffusion equations. *Applied mathematical modelling, 34*(10), 3071-3084. 1

[20] Sun, H., & Zhang, J. (2003). A high-order compact boundary value method for solving one-dimensional heat equations. *Numerical Methods for Partial Differential Equations: An International Journal, 19*(6), 846-857. 1

[21] Tatari, M., & Dehghan, M. (2010). A method for solving partial differential equations via radial basis functions: Application to the heat equation. *Engineering Analysis with Boundary Elements, 34*(3), 206-212. 1

[22] Li, X., & Wu, B. (2013). New algorithm for nonclassical parabolic problems based on the reproducing kernel method. *Mathematical Sciences, 7*(1), 1-5. 1

[23] Zhou, Y., Cui, M., & Lin, Y. (2009). Numerical algorithm for parabolic problems with non-classical conditions. *Journal of Computational and Applied Mathematics, 230*(2), 770-780. 1, 5, 4

[24] Zhu, C. G., & Kang, W. S. (2010). Numerical solution of BurgersFisher equation by cubic B-spline quasi-interpolation. *Applied Mathematics and Computation, 216*(9), 2679-2686. 1

[25] Zhu, C. G., & Wang, R. H. (2009). Numerical solution of Burgers equation by cubic B-spline quasi-interpolation. *Applied Mathematics and Computation, 208*(1), 260-272. 1